Pharmacokinetics and Metabolism of ^{14}C-Brivaracetam, a Novel SV2A Ligand, in Healthy Subjects

Maria Laura Sargentini-Maier, Pascal Espié, Alain Coquette, and Armel Stockis

UCB Pharma SA, Braine-l'Alleud, Belgium (M.L.S.-M., P.E., A.S.); and SGS Healthcare Services SA, Wavre, Belgium (A.C.)

ABSTRACT:

This study was designed to investigate the human absorption, disposition, and mass balance of ^{14}C-brivaracetam, a novel high affinity SV2A ligand with potent anticonvulsant activity. Six healthy male subjects received a single p.o. dose of ^{14}C-brivaracetam (150 mg, 82 μCi, or 3.03 MBq). Serial blood and complete urine and feces were collected until 144 h postdose. Expired air samples were obtained until 24 h. Brivaracetam was rapidly absorbed, with C_{max} of 4 μg/ml occurring within 1.5 h of dosing. Unchanged brivaracetam amounted to 90% of the total plasma radioactivity, suggesting a modest first-pass effect. Plasma protein binding of radioactivity was low (17.5%). Urinary excretion exceeded 90% after 2 days, and the final mass balance reached 96.8% of the radioactivity in urine and 0.7% in feces. Only 8.6% of the radioactive dose was recovered in urine as unchanged brivaracetam, the remainder being identified as non–cytochrome P450 (P450)- and P450-dependent biotransformation products resulting from hydrolysis of the amide moiety (M9, 34.2%), hydroxylation of the *n*-propyl side chain (M1b, 15.9%), and a combination of these two pathways leading to the hydroxy acid (M4b, 15.2%). Minor amounts of taurine and glucuronic acid conjugates and other oxidized derivatives were also identified. Brivaracetam is completely absorbed, is weakly bound to plasma proteins, extensively biotransformed through several metabolic pathways, and eliminated renally.

Brivaracetam is a novel ligand of the synaptic vesicle protein SV2A with a 10-fold higher affinity than levetiracetam (Kenda et al., 2004). A correlation between binding affinity for the SV2A site and antiseizure protection in the mouse audiogenic seizure model has been shown for a series of levetiracetam analogs (Lynch et al., 2004). Furthermore, brivaracetam dose-dependently inhibits voltage-dependent sodium currents (Zona et al., 2004) and reverses the inhibitory effects of negative modulators on γ-aminobutyric acid- and glycine-induced currents (Rigo et al., 2004). Preclinical in vivo and in vitro studies with brivaracetam have shown that it induces a more potent and complete suppression of seizure activity in experimental models of epilepsy (Matagne et al., 2003a; Kenda et al., 2004). Brivaracetam revealed pharmacological activity with ED_{50} in the range of 1.2 to 2.6 mg/kg administered i.p. in three rodent models of epilepsy (corneal-kindled mice, audiogenic-susceptible mice, and Genetic Absence Rats from Strasbourg) (Matagne et al., 2003b), corresponding to predicted human equivalent doses of 70 to 160 mg/day using body weight or 6 to 25 mg/day using body surface extrapolation. The clinical safety, tolerability, and pharmacokinetics of brivaracetam have been extensively studied in healthy human subjects (Rolan et al., 2004; Sargentini-Maier et al., 2007). The maximum tolerated dose was 1000 mg after a single p.o. dose and >800 mg/day after 2 weeks of multiple dosing. Brivaracetam was rapidly absorbed p.o.; food did not affect

the extent of absorption; its distribution volume amounted to the total volume of body water; and plasma half-life was between 7 and 8 h (Rolan et al., 2004; Sargentini-Maier et al., 2007). A proof of concept study in photosensitive epileptic patients confirmed the potent antiepileptic activity of the compound (Kasteleijn-Nolst Trenité et al., 2007), as evidenced by complete suppression of photoparoxysmal response lasting more than 2 days in all the patients after a single dose of 80 mg.

The objectives of the present study were to characterize the absorption, metabolism, disposition, and mass balance of a single 150-mg p.o. dose of ^{14}C-brivaracetam in healthy male subjects.

Materials and Methods

Reference Substances and Chemicals. Brivaracetam (M7) and the metabolite synthetic standards, (2*S*)-2-[(4*R*)-2-oxo-4-(2-(*R*)-hydroxy-propyl)-pyrrolidin-1-yl]-butanamide (M1a), (2*S*)-2-[(4*R*)-2-oxo-4-(2-(*S*)-hydroxy-propyl)pyrrolidin-1-yl]-butanamide (M1b), (2*S*)-2-[(4*R*)-2-oxo-4-(2-oxopropyl)-pyrrolidin-1-yl]-butanamide (M3), and (2*S*)-2-[(4*R*)-2-oxo-4-propylpyrrolidin-1-yl]-butanoic acid (M9) were synthesized by UCB Pharma (Braine-l'Alleud, Belgium). [^{14}C]Brivaracetam, labeled on the carbonyl position of the pyrrolidone ring, was obtained from Amersham Biosciences (Chalfont St. Giles, Bucks, UK). Liquid scintillation mixtures were from Canberra-Packard Benelux (Zellik, Belgium). All the other commercially available reagents and solvents were of either analytical or high-performance liquid chromatography (HPLC) grade.

Clinical Study. The study was conducted at the SGS Clinical Research Unit, Stuyvenberg Hospital (Antwerp, Belgium). The study protocol and the dosimetry calculations were approved by the Medical Ethics Committee of the

---

ABBREVIATIONS: Brivaracetam, (2*S*)-2-[(4*R*)-2-oxo-4-propylpyrrolidinyl] butanamide; HPLC, high-performance liquid chromatography; Ht, hematocrit; MS, mass spectrometry; TFA, trifluoroacetic acid; MDA, minimum detectable activity; CID, collision-induced dissociation; AUC_{0-t}, area under the plasma concentration-time curve from time of dosing to time of last measurable concentration; AUC, area under the plasma concentration-time curve; COSY, correlation spectroscopy; P450, cytochrome P450.

TABLE 1

Individual and mean (S.D.) cumulative excretion of ^{14}C-brivaracetam (% dose) until 144 h postdose (n = 6)

| | Subject | | | | | | Mean (S.D.) |
	1	2	3	4	5	6	
Urine	97.9	96.6	96.1	96.3	97.6	96.4	96.8 (0.7)
Feces	0.527	0.951	0.571	0.545	0.723	0.928	0.71 (0.19)
Air	N.D.	N.D.	N.D.	N.D.	N.D.	N.D.	
Total	98.4	97.6	96.7	96.8	98.3	97.3	97.5 (0.7)

N.D., not detected.

public hospitals of the city of Antwerp. The trial was conducted according to the recommendations described in the Declaration of Helsinki. Written informed consent was obtained from each subject before the start of the trial, after being informed of the nature and implications of the study.

The tissue distribution in nonpigmented and pigmented rats allowed the conclusion that the p.o. administration of 2.9 MBq (79 μCi) of ^{14}C-brivaracetam would result in a committed effective dose of 0.1 mSv, placing this trial at the upper limit of Risk Category I (ICRP Publication 60, 1991; ICRP Publication 62, 1993), namely, one tenth of the maximum permissible dose in this type of trial (category IIa, 1 mSv). Brivaracetam was dissolved in ethanol together with ^{14}C-brivaracetam in suitable proportions to obtain a specific radioactivity of approximately 20 KBq/mg (0.54 μCi/mg). The solution was evaporated to dryness, and 150 mg of powder was accurately weighed (to the nearest 0.1 mg) into hard gelatin capsules without excipients. The amount per capsule, the specific radioactivity of the labeled drug substance, the total radioactivity per capsule, and the isotopic purity were controlled shortly before use.

After an overnight fast, six healthy male subjects took one capsule containing 150 mg of ^{14}C-brivaracetam with 240 ml of water. The participants remained in upright position for 1 h. Food was withheld until 4 h postdose. Standardized meals were provided according to a fixed schedule. The subjects remained confined in the unit for the first 8 days of the study or until at least 95% of the radioactive dose was excreted.

Blood samples were collected in heparin-containing tubes before dosing and at 0.25, 0.5, 1, 1.5, 2, 3, 4, 6, 9, 12, 24, 36, 48, 72, 96, 120, and 144 h postdose. For metabolite identification and ex vivo radioactivity protein binding measurements, additional blood samples were collected from each subject at 1, 12, and 24 h postdose. Aliquots of 1 ml were kept for the determination of

radioactivity in whole blood, and the remainder was centrifuged at 4°C. Plasma samples were obtained by centrifugation (10 min, 2000g, 4°C) and transferred into polypropylene tubes for the determination of total radioactivity, for the determination of the parent compound, and for metabolic profiling. Hematocrit was determined once daily in the morning. Expired air was collected at predose and 0.5, 1, 1.5, 2, 3, 4, 6, 9, 12, and 24 h postdose: subjects were requested to blow through a glass straw into a vial containing 4 ml of a 1:1 mixture of Hyamine 10× hydroxide and 96% ethanol containing 0.02% phenolphthalein until persistent bleaching of the indicator. The amount of alkaline reagent was calculated to trap 1 mmol of carbon dioxide. Cumulative excretion was calculated assuming a carbon dioxide production of 1 kg/day or 947 mmol/h in humans.

All the urine emissions were collected in fractions at predetermined intervals: predose, 0 to 6, 6 to 12, 12 to 24, 24 to 48, 48 to 72, 72 to 96, 96 to 120, and 120 to 144 h. All the postdose stools were collected in stomacher bags (Seward Medical, London, UK) placed in tared plastic jars. Blood and air samples were stored at +4°C, and all the other samples were stored at −20°C until submitted to analytical determinations.

Radioactivity Determinations. Radioactivity in blood, plasma, urine, feces, and expired air was determined using a liquid scintillation counter (Tri-Carb model 2900TR, Canberra-Packard Benelux). The total radioactivity in plasma and blood was expressed as microgram-equivalents per milliliter brivaracetam. For plasma and urine samples, two aliquots (0.5 and 1.0 ml, respectively) were mixed directly with 10 ml of Ultima Gold scintillation mixture followed by liquid scintillation counting. For expired air, the vials containing the trapped air were added with 9 ml of Hionic-Fluor, and the samples were counted. Feces were mixed with water (approximately 1:1) and homogenized using a Stomacher 400 apparatus (Seward Medical). At least four aliquots of fecal homogenates (approximately 100 mg) were combusted using a Sample Oxidizer model 307 (Canberra-Packard Benelux). Radioactivity in the combustion products was determined by trapping the liberated $^{14}CO_2$ in various proportions of Carbo-Sorb-E absorbing reagent (PerkinElmer, Boston, MA) followed by liquid scintillation counting using Permafluor E scintillation mixture (PerkinElmer). For blood samples, two 0.25-ml aliquots were combusted and measured in a similar manner to that of the fecal homogenates. The radioactivity in blood cells was calculated from hematocrit (Ht) and from whole blood and plasma radioactivity using the equation: $C_{cell} = [C_{blood} - C_{plasma} \times (1 - Ht)]/Ht$.

Determination of Plasma Protein Binding. The ex vivo plasma protein binding of radioactivity was determined by equilibrium dialysis. Plasma sam-
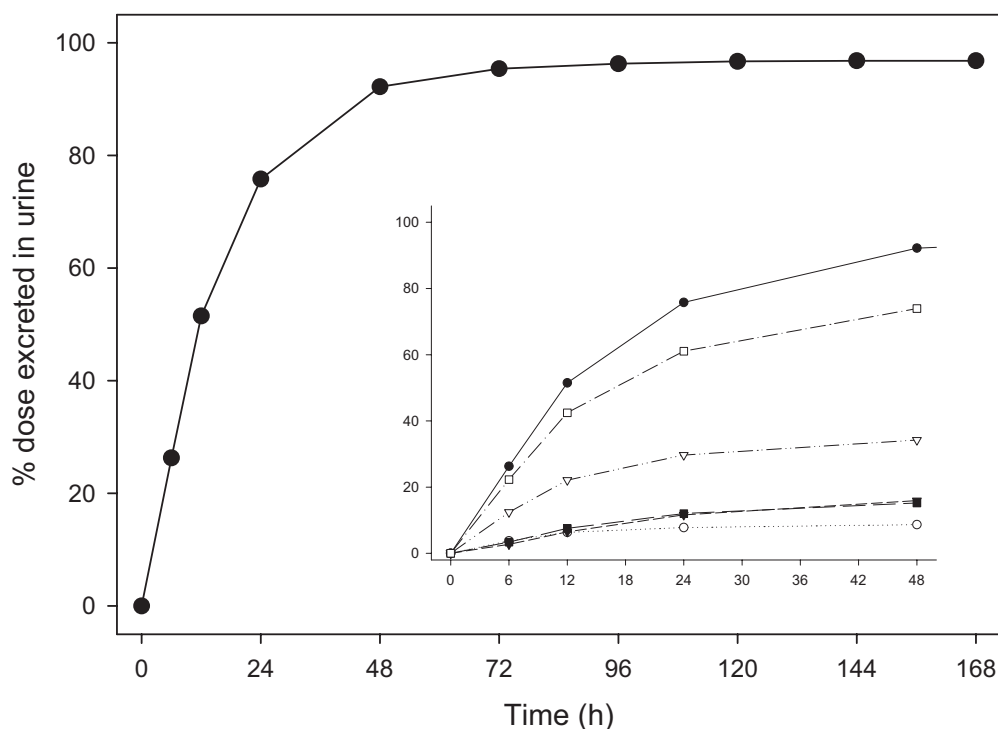

FIG. 1. Mean cumulative urinary excretion of total radioactivity (●), brivaracetam (○), M1b (▼), M9 (▽), M4a (■), and sum of brivaracetam and metabolites (□) after 150-mg single p.o. dose of ^{14}C-brivaracetam (n = 6).
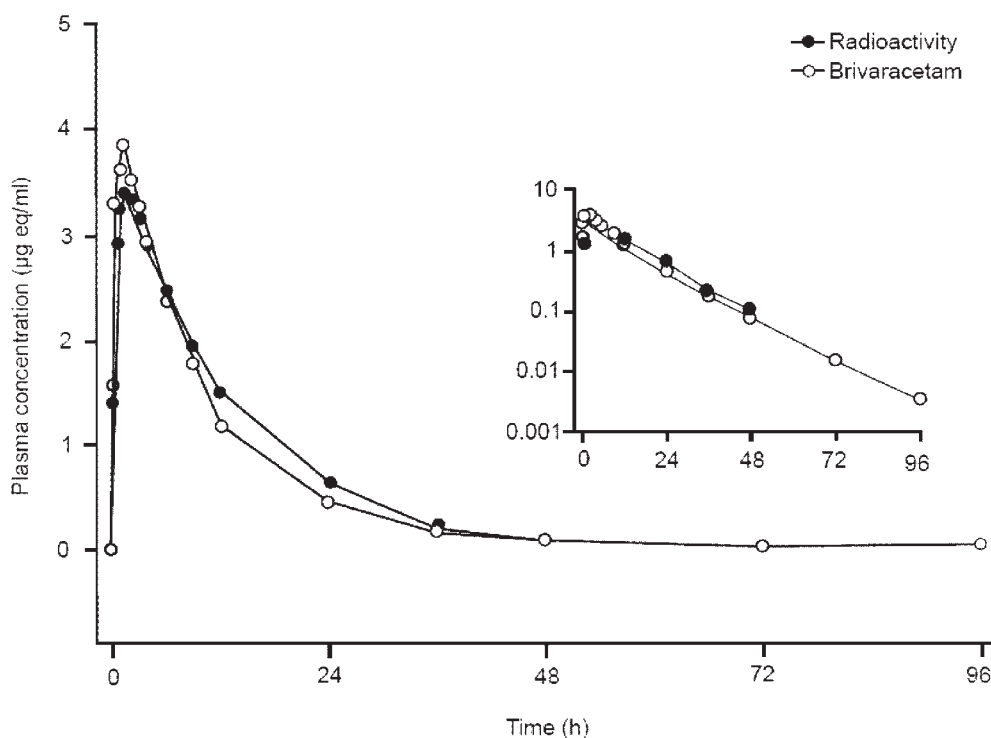
Fig. 2. Mean plasma concentration-time profiles of total radioactivity and brivaracetam after 150-mg single p.o. dose of ^{14}C-brivaracetam ($n = 6$).

TABLE 2

Plasma pharmacokinetic parameters (mean $\pm$ S.D.) of total radioactivity and brivaracetam after a single 150-mg p.o. dose of ^{14}C-brivaracetam ($n = 6$)

Parameter	Total Radioactivity	Brivaracetam
C_{max} (μg/ml)	3.6 ± 0.4	4.0 ± 0.5
T_{max} (h)^a	1.5 (0.25–2)	1.5 (0.25–2)
AUC_{0-t} (μg/ml)	48.9 ± 7.9	43.4 ± 10.8
AUC (μg/ml)	49.8 ± 8.3	44.6 ± 11.3
CL/F (ml/min/kg)		0.77 ± 0.19
Vz/F (ml/kg)		0.49 ± 0.05
$t_{1/2}$ (h)	8.8 ± 1.5	7.6 ± 1.7

^{a} Median (range).

TABLE 3

Radiometabolite quantification (% of plasma radioactivity – median, minimum-maximum) in plasma at 1.5, 6, and 12 h

Compound	1.5 h	6 h	12 h
M1b	N.D.	N.D. (N.D.–8.4)	6.0 (N.D.–15.5)
M7 (brivaracetam)	96.7 (91.7–97.4)	91.0 (87.2–93.2)	88.8 (78.7–100)
M9	1.6 (N.D.–5.5)	3.2 (N.D.–6.7)	N.D.

N.D., not detected (<82.4 cpm).

ples (1 ml) were dialyzed in triplicate at 37°C during 4 h using a Dianorm dialysis apparatus (Diachema AG, Zurich, Switzerland) and Spectra/Por membranes (membrane area = 4.5 cm^2; molecular weight cutoff = 12,000–14,000; Spectrum Inc., Houston, TX). Dialyzed plasma and buffer were mixed with 10 ml of Emulsifier Scintillator Plus scintillation mixture (PerkinElmer) and submitted to liquid scintillation counting. The percent binding of radioactivity to plasma proteins was expressed as follows: Binding (%) = 100 $\times$ (C$_{plasma}$ − C$_{buffer}$)/C$_{plasma}$.

Quantification of Brivaracetam in Plasma. Brivaracetam was determined in plasma samples after prepurification on solid-phase extraction cartridges using a previously described liquid chromatography/mass spectrometry (MS) method with electrospray ionization (Sargentini-Maier et al., 2007). The lower limit of quantification was 0.05 μg/ml.

Sample Preparation for Metabolite Profiling and Structural Elucida-

tion. Plasma samples (1 ml) were diluted with 1 ml of water containing 0.2% v/v trifluoroacetic acid (TFA), vortexed, diluted with 1 ml of methanol, vortexed, and diluted again with 1 ml of acetonitrile. After centrifugation and separation of the supernatant, the pellet was washed. The supernatant and the pellet wash were subsequently pooled, evaporated to dryness, and the residue reconstituted with 500 μl of water, containing 5% v/v acetonitrile before analysis. Urine samples were centrifuged to remove insoluble material before analysis.

Metabolic Profiling. All the urine samples from 0 to 6, 6 to 12, 12 to 24, and 24 to 48 h postdose and all the plasma samples until 24 h postdose were analyzed individually as collected. The radio-HPLC system consisted of an Agilent 1100 series chromatograph (Agilent Technologies, Diegem, Belgium) coupled to a Radiomatic 515 TR radiochemical detector (Canberra-Packard). The separation was performed on an Inertsil ODS-3 column (250 $\times$ 4.6 mm, 5 μm; GL Sciences, Tokyo, Japan) protected by an Inertsil ODS-3 guard column and thermostatically regulated at 40°C. The eluents were (A) 0.1% aqueous TFA (adjusted to pH 2.4 with aqueous ammonia) and 5% acetonitrile and (B) 0.1% aqueous TFA (pH 2.4) and 90% acetonitrile, at a total flow rate of 1 ml/min. A gradient was programmed from 0 to 35% of B in 70 min followed by 15 min at 100% B. A UV detector (220 nm) was inserted upstream of the radiochemical detector for recording retention times of the reference standards. The radiochemical detector cell had a volume of 1 ml for urine and 2 ml for plasma and received Ultima-Flo M scintillation mixture (Perkin-Elmer) at a flow rate of 3 ml/min. The background to be subtracted (Bs) from a radio-HPLC analysis was evaluated as follows: Bs = [Bm/N + 2x (Bm/N) 0.5] $\times$ N, where Bm is the measured background and N the number of samplings per minute. For the reported analyses, the measured backgrounds for the different counting cells were 9.4 cpm (1 ml of counting cell) and 14.2 cpm (2 ml of counting cell). The corresponding subtracted backgrounds were 28.8 and 38.0 cpm. The efficiency has been checked to be constant over the entire gradient (i.e., relative standard deviation = 2.4%). The minimum detectable activity (MDA) was calculated as follows: MDA = Bm $\times$ peak width/Tr, where Tr is the residence time in the counting cell. In plasma and urine, the MDA was 82.4 and 109 cpm, respectively.

Metabolite Structural Elucidation. The mass spectrometer was a Micromass tandem quadrupole time-of-flight QTOF2 instrument (Micromass, Manchester, UK) with dual electrospray source, operated by the Masslynx version 4.0 data system (Waters, Milford, MA). In full positive ion mode, the sample spray cone voltage was set at 20 V. The collision energy was 10 eV for
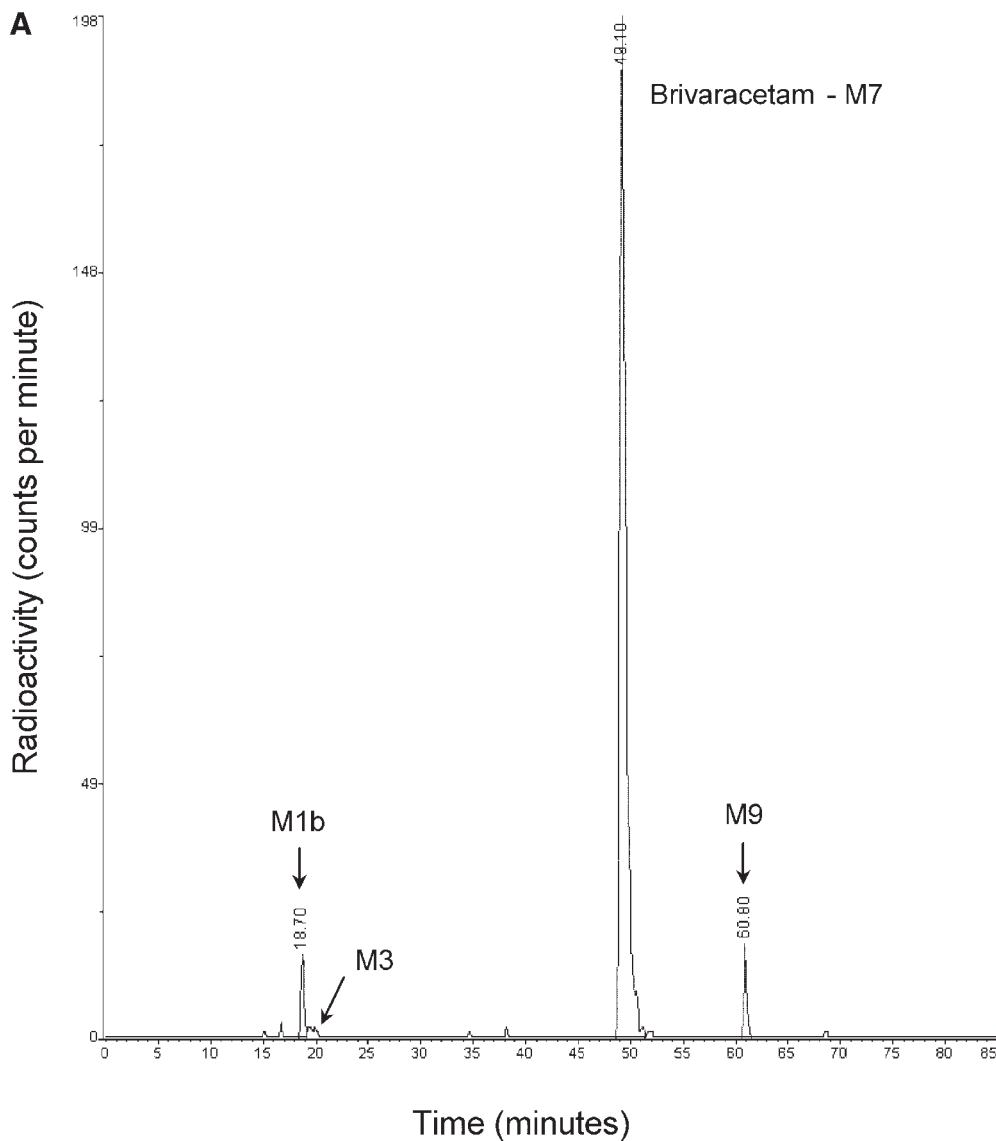
FIG. 3. A, representative radiochromatogram of circulating radioactivity (plasma at 6 h, subject 2). B, representative urine radiochromatogram (6–12-h interval, subject 2). The *y*-axis is effluent radioactivity in counts per minute (cpm), and the *x*-axis is elution time in minutes.
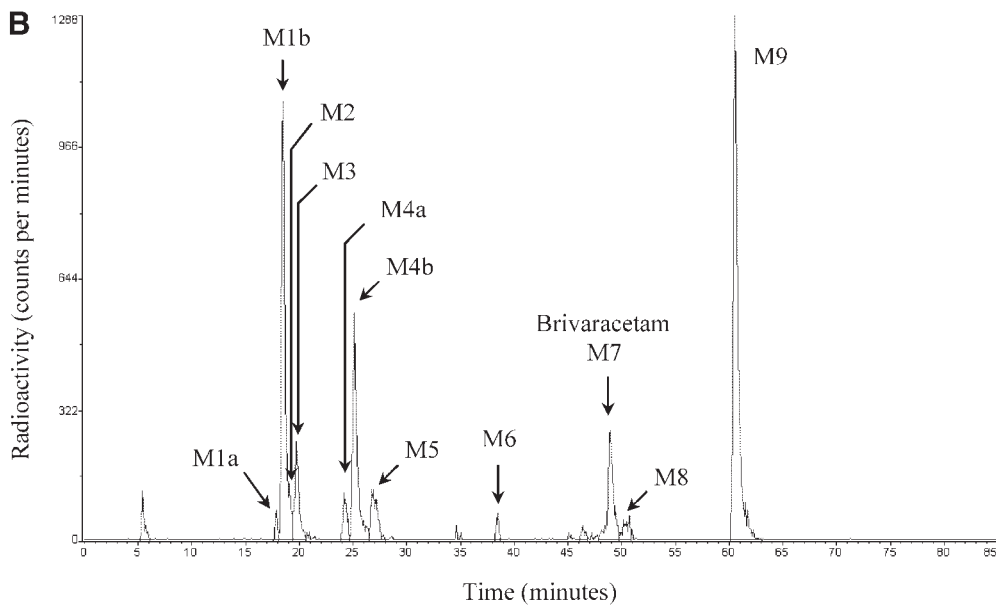
TABLE 4

Mean (S.D., n = 6) percentage of dose excreted in urine as radiometabolites over 48 h, proposed chemical structure, and accurate mass of the MH⁺ and MNa⁺ molecular ions and two major daughter ions
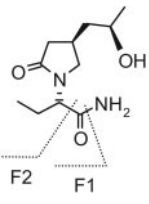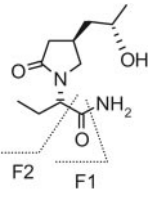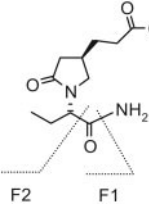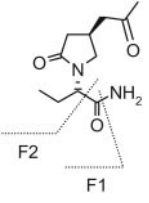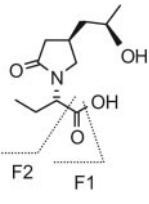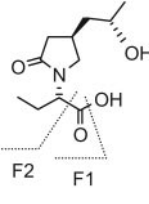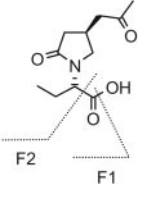
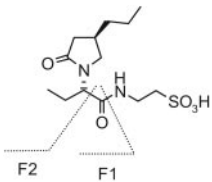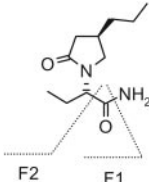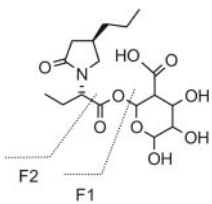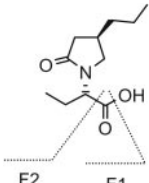| Compound	% in 0–48 h Urine (S.D.)	Structures	Calculated Mass and Error (milliunits)			
			MH$^+$	MNa$^+$	F1	F2
M1a	0.2		229.1552 (0.7)	251.1372 (0.4)	212.1287 (0.5)	184.1338 (0.6)
M1b	15.9 (7.4)		229.1552 (0.9)	251.1372 (−1.1)	212.1287 (−0.4)	184.1338 (−0.2)
M2	Traces		243.1345 (3.1)	265.1164 (1.2)	226.1079 (0.9)	198.1130 (0.0)
M3	3.5		227.1396 (0.1)	249.1215 (0.2)	210.1130 (0.3)	182.1181 (−0.1)
M4a (tentative)	2.8		230.1392 (−0.2)	252.1212 (0.7)	212.1287 (0.8)	184.1338 (0.4)
M4b	15.2 (2.4)		230.1392 (0.7)	252.1212 (0.9)	212.1287 (1.2)	184.1338 (1.6)
M5	3.8		228.1236 (1.8)	250.1055 (3.8)	210.1130 (2.5)	182.1181 (2.0)

TABLE 4—*Continued.*

Compound	% in 0–48 h Urine (S.D.)	Structures	Calculated Mass and Error (milliunits)			
			MH$^+$	MNa$^+$	F1	F2
M6	1.0		321.1484 (1.0)	343.1304 (2.2)	196.1338 (1.9)	168.1388 (3.3)
M7 (brivaracetam)	8.6 (3.8)		213.1603 (1.7)	235.1422 (−1.7)	196.1338 (−1.8)	168.1388 (−0.6)
M8	2.4		390.1764 (1.7)	412.1584 (2.3)	214.1443 (0.4)	168.1388 (1.5)
M9	34.2 (6.1)		214.1443 (−1.4)	236.1263 (0.4)	196.1338 (0.0)	168.1388 (−0.3)

full-scan MS and collision-induced dissociation (CID) experiments. In CID mode, the resolution of the quadrupole filter was set to approximately 5 atomic mass units to enable the entrance of a complete isotope cluster into the collision hexapole. The HPLC system was operated under the same conditions as described for metabolic profiling.

Metabolites were identified by the accurate masses of their protonated molecular ion and of fragment ions generated in-source or by CID. Compounds M1a, M1b, M3, M7, and M9 were confirmed by comparison of their retention times with authentic reference standards.

Metabolite M4b was isolated and purified from 250 ml of 12- to 24-h urine from subject 2, and its structural identification was performed by ^{1}H NMR. The 250-ml urine sample was mixed with an equal volume of 0.1% aqueous TFA. An Oasis HLB SPE column (Waters) containing 6 g of packing was conditioned successively with 70 ml of MeOH and 35 ml of 0.1% aqueous TFA. The 500 ml of diluted urine was slowly loaded onto the SPE column. The radioactive peak of interest was not retained on the column and eluted in the effluent. The latter was adjusted to pH 2.4 with aqueous 20% TFA and reloaded on a conditioned 6-g Oasis HLB SPE column. The column was washed out with 20 ml of water containing 0.1% TFA. The metabolite was then eluted with 30 ml of acetonitrile/methanol 70:30, which was evaporated to dryness under vacuum. The residue was reconstituted in 5 ml of 5% acetonitrile in 0.1% aqueous TFA, pH 2.4. The sample was then subjected to semipreparative HPLC on an Inertsil ODS-3 (250 × 10 mm, 5 μm) column at a temperature of 40°C using the same gradient system as for metabolic profiling and a flow rate of 2.5 ml/min. Fractions were collected using an Agilent 220 fraction collector. Each fraction was counted by liquid scintillation and individually analyzed by radio-HPLC. The fractions of interest were reduced under nitrogen to 1 ml and reinjected, and the purified metabolite was collected from the column effluent while monitoring the signal of the radio-metric detector fitted with a 150-μl heterogeneous counting cell. The purity of the final fraction was checked by HPLC with radiometric and UV detection. The final sample was evaporated to dryness under nitrogen and reconstituted in deuterated acetonitrile. Structural determination was performed by ^{1}H NMR spectrometry on a Bruker DRX 400-MHz spectrometer.

Pharmacokinetic Analysis. Pharmacokinetic parameters were derived using standard noncompartmental methods (Kinetica 2000, version 3.0, Innaphase, Champ sur Marne, France). Maximum concentration (C_{max}) and peak time (T_{max}) were directly derived from the concentration-time profiles. The area under the plasma concentration-time curve from the time of dosing to the time of the last measurable concentration (AUC_{0-t}) was calculated by the linear trapezoidal rule and extrapolated to infinity (AUC) as $AUC_{0-t} + Ct/\lambda z$, in which λz, the first-order rate constant associated with the terminal elimination phase, was estimated by linear regression of time versus log concentration. The apparent half-life ($t_{1/2}$) of the terminal elimination phase was calculated as $\ln(2)/\lambda z$. The total amount of excreted radioactivity was the sum of the amount excreted in urine, feces, and air.

Results

The six male subjects who participated in the study had a mean age of 30.9 years (range 18.5–43.8 years) and a mean body weight of 78 kg (range 69–92 kg). The administered brivaracetam and radiocarbon doses were 150.2 ± 5.3 mg (mean ± S.D., $n = 6$) and 3.02 ± 0.11 MBq (81.6 ± 3 μCi). The radiochemical purity of brivaracetam was found to be 100%.

Mass Balance. The cumulative recovery of radiocarbon reached 97.5 ± 0.7% of the dose in 144 h (Table 1). Most of the radioactivity was recovered in urine (96.8 ± 0.7%) and less than 1% in feces. No radioactivity was detected in exhaled air. The mean cumulative re-

covery of total radioactivity in urine over time is graphically illustrated in Fig. 1.

Pharmacokinetics. The mean plasma concentration-time profiles of radiocarbon and unchanged brivaracetam are illustrated in Fig. 2. The peak plasma concentration was reached at 1.5 h postdose for both brivaracetam and radiocarbon (Table 2). The area under the radiocarbon concentration curve, 49.8 ± 8.30 μg Eq/ml, was only slightly higher than for unchanged brivaracetam, 44.6 ± 11.3 μg/ml (Table 2). The mean apparent half-lives ($t_{1/2}$) were also similar, namely, 8.8 ± 1.5 and 7.6 ± 1.7 h, respectively. The clearance and distribution volume of brivaracetam were 0.77 ± 0.19 ml/min/kg and 0.49 ± 0.05 l/kg. The ratios of blood cell to plasma radioactivity versus time were submitted to linear least-squares regression: the mean ($\pm$ S.D.) intercept and slope were 0.58 ± 0.07 and 0.002 ± 0.003 ($n = 6$).

Metabolite Profiling. The recovery for the urine sample preparation step was checked on early and late samples and found to be >95%. Similarly, the extraction recovery for plasma was >90%. The column recovery at the end of the gradient was 100% for both plasma and urine.

As evidenced in Table 3, brivaracetam was the predominant species in plasma at 1.5, 6, and 12 h postdose, amounting to approximately 90% of the total circulating radioactivity. Metabolite M9 was measurable in some individuals up to 6 h postdose and accounted for less than 10% of the circulating radioactivity, whereas metabolite M1b appeared later and reached 6% of the circulating radioactivity at 12 h (15.5% in one individual). Metabolites M3 and M4b were below the limit of detection at all the times (minimum detectable radioactivity, 82.4 cpm). A representative HPLC radiochromatogram of circulating metabolites is shown in Fig. 3A (subject 2, 6-h postdose sample).

Table 4 lists the mean percentages of each brivaracetam-related species excreted in the urine in the 0- to 48-h time interval, together with their assigned structure and characteristic molecular ions and two main fragmentation products. A representative radiochromatogram of urine (subject 2, 6–12-h time interval) is shown in Fig. 3B. The mean 48-h cumulative urinary excretion of the parent compound M7 was $8.6 \pm 3.8\%$ of the dose, whereas that of M9, M1b, and M4b amounted to 34.2 ± 6.1, 15.9 ± 7.4, and $15.2 \pm 2.4\%$ of the dose, respectively. All the other metabolites (M1a, M2, M3, M4a, M5, M6, and M8) were minor, each of them amounting for less than 5% of the dose.

Metabolite Identification. In addition to the parent drug, 10 metabolites were identified in the urine (Table 4).

Brivaracetam (M7) exhibited an MH$^+$ molecular ion at m/z 213. Fragment ions at m/z 196 and 168, issued respectively from a loss of NH_3 and NH_3+CO, indicated the presence of an amide group. Its identity was confirmed by comparison with the reference standard.

Metabolites M1a and M1b displayed a protonated molecular ion at m/z 229, 16u higher than the parent drug, suggesting isomeric monohydroxylated metabolites. Their full-scan mass spectra displayed the class-characteristic losses of an intact amide group with elimination of NH_3 at m/z 212 followed by a consecutive loss of CO to generate a signal at m/z 184. The high-resolution mass to charge ratios of the molecular ion and of the characteristic fragments were identical for M1a and M1b (Table 4).

Metabolite M2 eluted in the front part of the M3 peak. The full-scan mass spectrum of metabolite M2 showed a protonated molecule at m/z 243, 30u higher than the parent drug, suggesting the formation of a carboxylic acid group. Fragment ions at m/z 226 and 198, issued respectively from a loss of NH_3 and NH_3+CO, indicated that the amide group present on the parent drug was intact. The CID product ion mass spectrum of the deprotonated molecule (m/z 241) suggested the presence of a carboxylic acid group on the propyl chain. Accurate mass measurement results in CID mode revealed class-characteristic

losses of H_2O (m/z 223) and CO_2 (m/z 197) from the deprotonated molecule and indicated a carboxylic acid group. Moreover, an abundant fragment ion at m/z 127 indicated an intact butyramide moiety. Based on these data, M2 was tentatively identified as 2-[4-(3-carboxypropyl)-2-oxo-pyrrolidin-1-yl]-butyramide.

Metabolite M3 exhibited a protonated molecular ion at m/z 227, 14u higher than the parent drug, suggesting conversion of a CH_2 of the parent drug to a ketone. The full-scan mass spectrum indicated the class-characteristics losses of an intact amide group with elimination of NH_3 at m/z 210 along with a consecutive loss of CO at m/z 182. Based on these data, M3 was identified by comparison with the reference standard as incorporating the ketone group on the penultimate carbon of the propyl chain.

Metabolites M4a and M4b displayed a protonated molecular ion at m/z 230, 17u higher than the parent drug, suggesting isomeric monohydroxylated metabolites with the amide group hydrolyzed. Fragment ions at m/z 212 and 184, issued respectively from a loss of H_2O and H_2O+CO, indicated that the amide present on the parent drug had been hydrolyzed. The structure of metabolite M4b was also confirmed by high-field NMR after preparative chromatography isolation from urine and purification.

The 400-MHz ^{1}H,^{1}H-correlation spectroscopy (COSY) spectrum of metabolite M4b is displayed in Fig. 4. The triplet at $\delta = 0.9$ ppm and the doublet at $\delta = 1.1$ ppm were assigned to methyl groups. By its multiplicity, the doublet indicated that it had only one vicinal proton and thus that the monohydroxylation took place on the penultimate carbon of one of the alkyl chains. That vicinal proton was identified as the sextuplet at $\delta = 3.7$ ppm by a cross-peak in the COSY spectrum. It was coupled to a triplet at $\delta = 1.5$ ppm as indicated by a cross-peak in the COSY spectrum. From its multiplicity and chemical shift, that signal was assigned to the methylene in position 1 on the propyl chain, confirming that the hydroxylation took place on the propyl chain in ω-1 position. From the COSY spectrum, it can be seen that that triplet was integrated in the 2-oxo-4-propylpyrrolidinyl spin system. The second spin system of the molecule was associated to the unchanged butyramide chain. The particularity in that COSY spectrum was the doublet at $\delta = 1.3$ ppm correlated with the sextuplet at $\delta = 5.2$ ppm. Those were respectively assigned to the methyl and the methine of the alcohol moiety of a first molecule of M4b, forming an ester link with a second molecule of M4b. This dimer was found to be stable in pure acetonitrile but unstable in water. Based on these data, M4b was identified as the 2-[2-oxo-4-(2-hydroxypropyl)pyrrolidin-1-yl]butanoic acid. By analogy with the metabolites M1a and M1b, M4a was tentatively identified as the diastereoisomer of M4b.

Metabolite M5 displayed a full-scan mass spectrum with a protonated molecular ion at m/z 228, 15u higher than the parent drug, suggesting hydrolysis of the amide group and conversion of a CH_2 of the parent drug to a ketone. Fragment ions at m/z 210 and 182, issued respectively from a loss of H_2O and H_2O+CO, suggested that the amide group of the parent drug had been hydrolyzed. The CID product ion mass spectrum of the deprotonated molecule M5 displayed a loss of acetone, indicating that the ketone group was on the penultimate carbon of the propyl chain. Based on these data, M5 was tentatively identified as 2-[2-oxo-4-(2-oxo-propyl)pyrrolidin-1-yl]butanoic acid.

Metabolite M6 displayed a protonated ion at m/z 321, 107u higher than the carboxylic acid metabolite M9, suggesting a taurine conjugate. The full-scan mass spectrum displayed the class-characteristic fragment ions at m/z 196 issued from the loss of the taurine moiety and at m/z 168 issued from a subsequent loss of CO. From these data, M6 has been tentatively identified as the taurine conjugate of M9.
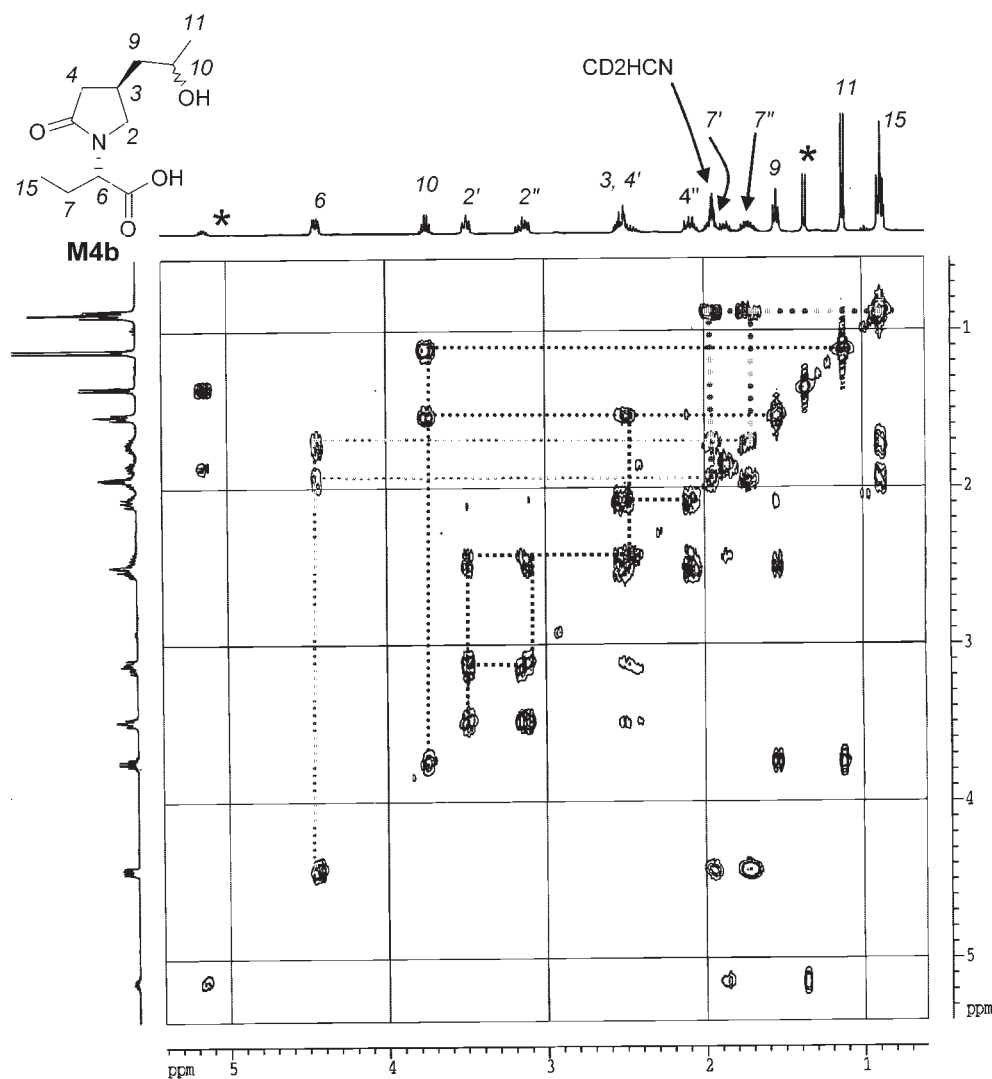
FIG. 4. Four hundred megahertz ^{1}H,^{1}H COSY spectrum of metabolite M4b after isolation and purification from urine. Annotated off-diagonal signals and dashed lines show proton-proton correlation. Solvent was CD$_3$CN. Asterisks indicate a putative dimer of M4b.

Metabolite M8 exhibited a protonated molecular ion at m/z 390, 176u higher than the metabolite issued from amide hydrolysis M9, suggesting a glucuronide conjugate. The full-scan mass spectrum indicated the class-characteristic fragment at m/z 214 issued from the loss of dehydroglucuronic acid (-176u) and 168 from the loss of CO. Based on these data, M8 was tentatively identified as an ester glucuronide of M9.

Metabolite M9 displayed a protonated molecular ion at m/z 214, 1u higher than the parent drug, suggesting the hydrolysis of the amide group to a carboxylic acid. Fragment ions at m/z 196 and 168, issued respectively from a loss of H$_2$O and H$_2$O+CO, indicated that the amide group present on the parent drug had been hydrolyzed. M9 was also identified by comparison with the reference standard. The overall biotransformation scheme of brivaracetam is illustrated in Fig. 5.

Ex Vivo Protein Binding. The nonspecific binding of radioactivity to the dialysis apparatus seemed to be insignificant, and the time to reach equilibrium was 4 h. The concentrations of radioactivity in the analyzed plasma ranged from 410 to 3600 ng Eq/ml: within this concentration range, the protein binding was independent of the initial concentration. The average (S.D.) plasma protein binding at 1, 12, and 24 h postdose was 18.7 $\pm$ 1.7, 17.6 $\pm$ 2.0, and 16.2 $\pm$ 3.5%, respectively.

Discussion

The objective of the present study was to characterize the absorption, metabolism, disposition, and mass balance of a single 150-mg p.o. dose of radiocarbon-labeled brivaracetam, and to identify its biotransformation pathways in humans. Mass balance was achieved, with a mean total recovery of radioactivity of 97.5%. Radioactivity was almost completely excreted in urine, accounting for 96.8% of the dose, whereas the radioactivity excreted in feces was <1%. No radioactivity was detectable in exhaled air.

Brivaracetam accounted for only 8.6% of the dose excreted in urine, indicating extensive biotransformation. However, unchanged brivaracetam represented the predominant circulating component (plasma AUC ratio to radioactivity ~90%).

The mean blood cell-to-plasma radioactivity ratio of 0.58 and the negligible change over time (~10% in 24 h) suggested some distribution in blood cells, reaching rapid equilibrium, and the absence of accumulation of brivaracetam or metabolites.

The plasma protein binding, 17.5% on average, was neither concentration- nor time-dependent. Because the bulk of plasma radioactivity was assigned to brivaracetam, this figure closely approximates the protein binding of the unchanged drug.

In vitro studies have shown that brivaracetam is slowly oxidized by liver microsomes and human hepatocytes (Whomsley et al.,
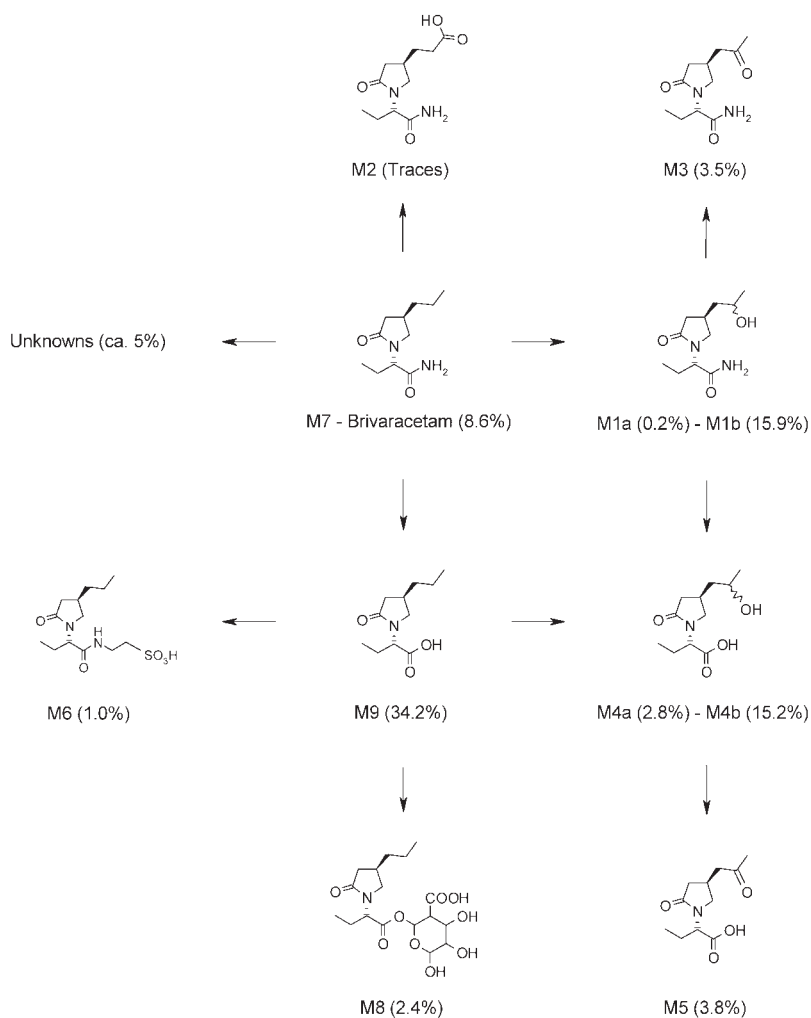
FIG. 5. Proposed metabolic pathways of brivaracetam in humans (mean percentage dose recovered in urine within 48 h).

2007). In this study, 10 metabolites issued from hydrolysis, oxidation, and conjugation of brivaracetam were identified. Brivaracetam (M7) and four metabolites for which authentic standards were available (M1a, M1b, M3, and M9) were confirmed by their chromatographic retention times and high-resolution mass spectra. The structure of M4b was assigned based on high-resolution mass spectral and proton NMR data. By analogy with M1a/M1b, M4a was tentatively identified as the diastereoisomer of M4b. The chemical structures of other metabolites were tentatively assigned based on mass spectral data only.

The proposed scheme for the biotransformation pathways of brivaracetam in humans is illustrated in Fig. 5. The major route of metabolism is the hydrolysis of the acetamide moiety, leading to the carboxylic acid metabolite M9 (34% of the dose in urine). The other major metabolic pathways are the oxidation of the propyl chain, leading to M1b (16% of the dose in urine) and the product of the hydrolysis of M1b and/or oxidation of M9 to M4b (15% of the dose in urine). Other oxidized metabolites (M3 and M5) and conjugates with glucuronic acid (M8) or taurine (M6) played a minor role in the biotransformation of brivaracetam. Overall, the identified metabolites accounted for >87% of the radioactivity recovered in urine.

In human liver microsomes, the in vitro and in vivo intrinsic clearances for production of M1b from brivaracetam were low. The extrapolated hepatic clearance (0.16 ml/min/kg) represented only 20% of the total in vivo clearance, suggesting a low potential for interference with brivaracetam metabolism through inhibition of cytochrome P450 (P450)-mediated metabolism. The principal P450 isoform responsible for the production of M1b is CYP2C8, with minor contributions from CYP3A4, CYP2C19, and possibly CYP2B6 (Whomsley et al., 2007).

The enzymes responsible for the production of the acidic metabolites M9 and M4b are unknown, although it is speculated that the hydrolysis of the acetamide moiety is mediated by high-capacity/low-affinity amide hydrolases similarly to levetiracetam, another member of the racetam family (Strolin Benedetti et al., 2003). Whether the hydroxy acid M4b is formed by hydrolysis to M9 followed by oxidation, or by oxidation to M1b followed by hydrolysis is also unknown and deserves further investigation.

In conclusion, this study has shown that brivaracetam is completely absorbed, is weakly bound to plasma proteins, is extensively metabolized through several non–P450- and P450-dependent pathways and is entirely eliminated renally. Therefore, the biotransformation of brivaracetam is unlikely to be importantly altered by clinical drug interactions. However, characterization of the enzymes involved in its metabolism warrants further investigations.

References

ICRP Publication 60 (1991) 1990 *Recommendations of the International Commission on Radiological Protection,* Pergamon Press, Oxford, UK.

ICRP Publication 62 (1993) *Radiological Protection in Biomedical Research,* Pergamon Press, Oxford, UK.

Kasteleijn-Nolst Trenité DGA, Genton P, Parain D, Masnou P, Steinhoff BJ, Jacobs T, Pigeolet E, Stockis A, and Hirsch E (2007) Evaluation of brivaracetam, a novel SV2A ligand, in the photosensitivity model. *Neurology* **69:**1027–1034.

Kenda BM, Matagne AC, Talaga PE, Pasau PM, Differding E, Lallemand BI, Frycia AM, Moureau FG, Klitgaard HV, Gillard MR, et al. (2004) Discovery of 4-substituted pyrrolidone butanamides as new agents with significant antiepileptic activity. *J Med Chem* **47:**530–549.

Lynch BA, Lambeng N, Nocka K, Kensel-Hammes P, Bajjalieh SM, Matagne A, and Fuks B (2004) The synaptic vesicle protein SV2A is the binding site for the antiepileptic drug levetiracetam. *Proc Natl Acad Sci U S A* **101:**9861–9866.

Matagne A, Kenda B, Michel P, and Klitgaard H (2003a) UCB 34714, a new pyrrolidone derivative: comparison with levetiracetam in animal models of chronic epilepsy in vivo. *Epilepsia* **44 (Suppl 9):**260–261.

Matagne A, Kenda B, Michel P, and Klitgaard H (2003b) UCB 34714, a new pyrrolidone derivative, suppresses seizures epileptogenesis in animal models of chronic epilepsy in vivo. *Epilepsia* **44 (Suppl 8):**53–54.

Rigo JM, Nguyen L, Hans G, Belachew S, Moonen G, Matagne A, and Klitgaard H (2004) UCB 34714: effect on inhibitory and excitatory neurotransmission. *Epilepsia* **45 (Suppl 3):**56.

Rolan P, Pigeolet E, and Stockis A (2004) UCB 34714: single and multiple rising dose safety, tolerability, and pharmacokinetics in healthy subjects. *Epilepsia* **45 (Suppl 7):**314–315.

Sargentini-Maier ML, Rolan P, Connell J, Tytgat D, Jacobs T, Pigeolet E, Riethuisen JM, and Stockis A (2007) Brivaracetam safety, tolerability, pharmacokinetics and CNS pharmacodynamic effects after 10 to 1400 mg single rising oral doses in healthy males. *Br J Clin Pharmacol* **63:**680–688.

Strolin Benedetti M, Whomsley R, Nicolas JM, Young C, and Baltes E (2003) Pharmacokinetics and metabolism of 14C-levetiracetam, a new antiepileptic agent, in healthy subjects. *Eur J Clin Pharmacol* **59:**621–630.

Whomsley R, Brochot A, Dell'Aiera S, Delepine X, and Espié P (2007) Identification of the cytochrome P450 isoforms responsible for the hydroxylation of brivaracetam (Abstract). *AAPS Journal* **9(Suppl 2):**T3408.

Zona C, Pieri M, Klitgaard H, and Margineanu D-G (2004) UCB 34714, a new pyrrolidone derivative, inhibits Na$^+$ currents in rat cortical neurons in culture. *Epilepsia* **45 (Suppl 7):**146.

Address correspondence to: M. L. Sargentini-Maier, UCB Pharma SA, Chemin du Foriest, B-1420 Braine-l'Alleud, Belgium. E-mail: laura.maier@ucb-group.com